

# CUQ-GNN: Committee-based Graph Uncertainty Quantification using Posterior Networks

Clemens Damke<sup>1</sup> (✉) and Eyke Hüllermeier<sup>1,2</sup>

<sup>1</sup> Institute of Informatics, LMU Munich, Germany  
{clemens.damke, eyke}@ifi.lmu.de

<sup>2</sup> Munich Center for Machine Learning (MCML), Germany

**Abstract** In this work, we study the influence of domain-specific characteristics when defining a meaningful notion of predictive uncertainty on graph data. Previously, the so-called *Graph Posterior Network* (GPN) model has been proposed to quantify uncertainty in node classification tasks. Given a graph, it uses *Normalizing Flows* (NFs) to estimate class densities for each node independently and converts those densities into Dirichlet pseudo-counts, which are then dispersed through the graph using the *personalized Page-Rank* (PPR) algorithm. The architecture of GPNs is motivated by a set of three axioms on the properties of its uncertainty estimates. We show that those axioms are not always satisfied in practice and therefore propose the family of *Committee-based Uncertainty Quantification Graph Neural Networks* (CUQ-GNNs), which combine standard *Graph Neural Networks* (GNNs) with the NF-based uncertainty estimation of *Posterior Networks* (PostNets). This approach adapts more flexibly to domain-specific demands on the properties of uncertainty estimates. We compare CUQ-GNN against GPN and other uncertainty quantification approaches on common node classification benchmarks and show that it is effective at producing useful uncertainty estimates.

**Keywords:** uncertainty quantification, graph neural networks

## 1 Introduction

In machine learning systems, particularly those where safety is important, accurately quantifying prediction uncertainty is paramount. One source of predictive uncertainty is the inherent stochasticity of the data-generating process, which is referred to as *aleatoric uncertainty* (AU) and cannot be reduced by sampling additional data. For example, when tossing a fair coin, the outcome is uncertain, and this uncertainty is of purely aleatoric nature. *Epistemic uncertainty* (EU), on the other hand, arises from a lack of knowledge about the data-generating process. It can be reduced by collecting more data and should vanish in the limit of infinite data [23]. For example, the lack of knowledge about the bias of a coin is of epistemic nature, and it increases the (total) uncertainty about the outcome of a coin toss. This uncertainty, however, can be reduced by tossing the coin repeatedly and estimating the bias from the outcomes.

In the context of graph data, the structural information is an additional contributing factor to the uncertainty, making *uncertainty quantification* (UQ) particularly challenging. In this paper, we will focus specifically on the problem of UQ for (semi-supervised) node classification. Applications of this problem include, for example, the classification of documents in citation networks [8, 38], or the classification of users or posts in social networks [40].

Recently, Stadler et al. [41] have proposed *Graph Posterior Networks* (GPNs) as an approach to UQ for node classification. In this paper, we provide a novel perspective on GPN motivated by the field of risk and decision analysis [11, 12]. More specifically, we show that GPN can be interpreted as an opinion pooling model employing the so-called *log-linear opinion pooling* (LLOP) scheme for structure-aware UQ (Section 3). Motivated by this interpretation, we describe the limitations of GPN and its axiomatic approach to UQ in general (Section 4). To address those limitations, we introduce the family of *Committee-based Uncertainty Quantification Graph Neural Network* (CUQ-GNN) models, which is motivated by the notion of *behavioral pooling*, combining standard *Graph Neural Networks* (GNNs) with the *Posterior Network* (PostNet). Then, we compare our behavioral CUQ-GNN model against the axiomatic GPN model (Section 5). The effectiveness of CUQ-GNN is demonstrated on multiple common node classification benchmarks.

## 2 Uncertainty Quantification

There are different formalizations of uncertainty in the literature on UQ. Depending on the desired properties of the uncertainty measure, different notions may be more or less suitable. We evaluate the adequacy of a measure of uncertainty through two lenses:

1. Its adherence to a set of axioms [9, 35, 37, 45].
2. Its performance on a predictive task, such as outlier detection [10].

Given our focus on UQ for the node classification setting, we start with a brief overview of uncertainty measures for classification tasks.

### 2.1 Entropy-based Uncertainty Measures

Predictions in  $K$ -class classification tasks are commonly represented in terms of probability distributions  $\theta = (\theta_1, \dots, \theta_K) \in \Delta_K$ , where  $\Delta_K$  represents the unit  $(K - 1)$ -simplex, and  $\theta_k$  denotes the probability of the  $k$ -th class. Thus, the true outcome (materialized class label)  $Y$  remains uncertain and can be seen as a matter of chance (aleatoric uncertainty). In addition, the prediction  $\theta$  itself is normally uncertain, too. This (epistemic) uncertainty of the learner can be represented through a second-order probability distribution  $Q$  on  $\Delta_K$ . Consequently, the true distribution over the  $K$  classes is viewed as a random variable  $\Theta \sim Q$ . Given a second-order distribution  $Q$ , its expectation is

$$\bar{\theta} := \mathbb{E}_Q[\Theta] = \int_{\Delta_K} \theta \, dQ(\theta). \quad (1)$$

The *total uncertainty* (TU) regarding the outcome  $Y$  is quantified by the Shannon entropy of  $\bar{\theta}$ :

$$\text{TU}(Q) := H(\mathbb{E}_Q[\theta]) = - \sum_{k=1}^K \bar{\theta}_k \log \bar{\theta}_k. \quad (2)$$

Furthermore, a breakdown of this uncertainty into aleatoric and epistemic components can be achieved through a well-established result from information theory, which states that entropy is the sum of conditional entropy and mutual information [15, 25]. This result suggests a quantification of *aleatoric uncertainty* (AU) as conditional entropy (of the outcome  $Y$  given the first-order distribution  $\Theta$ ):

$$\text{AU}(Q) := \mathbb{E}_Q[H(\Theta)] = - \int_{\Delta_K} \sum_{k=1}^K \theta_k \log \theta_k \, dQ(\theta). \quad (3)$$

Moreover, the *epistemic uncertainty* (EU) can then be defined as the difference between TU and AU:

$$\text{EU}(Q) := \text{TU}(Q) - \text{AU}(Q) = I(Y; \Theta) = \mathbb{E}_Q[D_{\text{KL}}(\Theta \parallel \bar{\theta})], \quad (4)$$

where  $I(\cdot; \cdot)$  denotes mutual information and  $D_{\text{KL}}(\cdot \parallel \cdot)$  the *Kullback-Leibler* (KL) divergence. Another entropy-based approach to quantify EU is via the differential entropy of the second-order distribution  $Q$  [29, 30]:

$$\text{EU}_{\text{SO}}(Q) := H(Q) = - \int_{\Delta_K} \log Q(\theta) \, dQ(\theta). \quad (5)$$

We will refer to this notion of EU as *second-order epistemic uncertainty*. Note that the differential entropy of  $Q$  can be negative, with  $-\infty$  representing a state of no uncertainty, i.e., a Dirac measure. However, some axiomatic characterizations of uncertainty assume that a state of no uncertainty is represented by an uncertainty of zero [45];  $\text{EU}_{\text{SO}}$  is therefore not without controversy. Apart from the entropy-based measures we just described, uncertainty is also often quantified in terms of other concentration measures, such as variance [16, 37], confidence or Dirichlet pseudo-counts. We will now briefly review the latter two notions of uncertainty.

## 2.2 Least-confidence and Count-based Uncertainty Measures

Given a second-order distribution  $Q$ , an alternative notion of uncertainty is provided by the so-called *least-confidence* of the expected distribution  $\bar{\theta}$ , defined as  $\text{LConf}(Q) := 1 - \max_k \bar{\theta}_k$ . Note the similarity of this measure to the TU measure in Eq. (2);  $\text{LConf}(Q)$  can therefore be seen as a measure of *total* uncertainty, too. However, in the literature this measure is also used as a proxy for *aleatoric* uncertainty [10].

Finally, if  $Q$  is described by a Dirichlet distribution  $\text{Dir}(\alpha)$ , where  $\alpha = (\alpha_1, \dots, \alpha_K)$  is a vector of pseudo-counts, the sum  $\alpha_0 = \sum_{k=1}^K \alpha_k$  describes how

concentrated  $Q$  is around the expected distribution  $\bar{\theta}$ . Thus, the EU encoded by a Dirichlet distribution  $Q$  can be quantified by  $\text{EU}_{\text{PC}}(Q) := -\alpha_0$ , which we will call *pseudo-count-based epistemic uncertainty* [10, 24, 28].

### 3 Posterior and Graph Posterior Networks

As just described, uncertainty can be formalized in various ways, and the selection of an uncertainty measure hinges upon the specific criteria it should satisfy. In graph-related contexts, an additional element contributing to uncertainty, namely structural information, requires formalization. Stadler et al. [41] propose an axiomatic approach to account for structure-induced uncertainty, called *Graph Posterior Network* (GPN). As mentioned in the introduction, GPNs are essentially a combination of PostNets [10] and the *approximate personalized propagation of neural predictions* (APPNP) node classification model [17]. We begin with a review of the PostNets and GPNs and the notions of uncertainty they provide.

#### 3.1 Posterior Networks

A PostNet is an *evidential deep learning* classification model [39], quantifying predictive uncertainty via a second-order distribution  $Q$ , learned through a second-order loss function  $L_2$ . A standard (first-order) loss function  $L_1 : \Delta_K \times \mathcal{Y} \rightarrow \mathbb{R}$  takes a predicted first-order distribution  $\hat{\theta} \in \Delta_K$  and an observed ground-truth label  $y \in \mathcal{Y}$  as input (where  $\mathcal{Y}$  denotes the set of classes); the *cross-entropy* (CE) loss is a common example of such a first-order loss function. Similarly, a second-order loss  $L_2$  takes a second-order distribution  $Q$ , i.e., a distribution over  $\Delta_K$ , as input, to which it again assigns a loss in light of an observed label  $y \in \mathcal{Y}$ . PostNet uses the so-called *uncertain cross-entropy* (UCE) loss [7], which is defined as

$$L_2(Q, y) := \mathbb{E}_Q [\text{CE}(\Theta, y)] = - \int_{\Delta_K} \log P(y | \theta) dQ(\theta). \quad (6)$$

However, directly minimizing a second-order loss, like the UCE loss, presents challenges, as the minimum is attained when  $Q$  is a Dirac measure concentrating all probability mass on  $\theta^* = \arg \min_{\theta \in \Delta_K} \text{CE}(\theta, y)$  [5]. Consequently, for the notions of EU we discussed in Section 2, the optimal  $Q^*$  will have no EU, i.e.,  $\text{EU} = 0$  (Eq. (4)) and  $\text{EU}_{\text{PC}} = -\infty$  (Section 2.2). To mitigate this issue, a regularization term, typically the differential entropy of  $Q$ , is added to the second-order loss function, incentivizing a  $Q$  that is less concentrated. Whether one can obtain a faithful representation of epistemic uncertainty has been generally questioned by Bengs et al. [6]. One should therefore be cautious when interpreting the EU estimates of evidential deep learning models, such as PostNet. We will not attempt to interpret uncertainty estimates in a quantitative manner but rather focus on the question of whether they are qualitatively meaningful, e.g.,

by considering whether anomalous or noisy instances can be identified via their uncertainty.

PostNet models the second-order distribution  $Q$  as a Dirichlet distribution  $\text{Dir}(\alpha)$ , where  $\alpha = (\alpha_1, \dots, \alpha_K)$  is a vector of pseudo-counts. The predicted pseudo-counts  $\alpha_k$  for a given instance  $\mathbf{x}^{(i)} \in \mathcal{X}$  are defined as

$$\alpha_k = 1 + \mu \cdot P\left(\mathbf{z}^{(i)} \mid y^{(i)} = k\right) \cdot P\left(y^{(i)} = k\right), \quad (7)$$

where  $\mathbf{z}^{(i)} = f(\mathbf{x}^{(i)}) \in \mathbb{R}^H$  is a latent neural network embedding of  $\mathbf{x}^{(i)}$  and  $\mu \in \mathbb{R}$  a so-called *certainty budget*, determining the highest attainable pseudo-count for a given instance. The class-conditional probability  $P(\mathbf{z}^{(i)} \mid k)$  by a normalizing flow model for the class  $k$  estimates the density of the instance. Overall, the PostNet model therefore consists of a neural network encoder model  $f$  and  $K$  normalizing flow models, one for each class.

### 3.2 Graph Posterior Networks

*Graph Posterior Networks* (GPNs) extend the PostNet model to the node classification problem in graphs. Let  $G := (\mathcal{V}, \mathcal{E})$  denote a graph, where  $\mathcal{V}$  is a set of  $N := |\mathcal{V}|$  nodes and  $\mathcal{E} \subseteq \mathcal{V}^2$  the set of edges. The adjacency matrix of  $G$  is denoted by  $\mathbf{A} = (A_{i,j}) \in \{0, 1\}^{N \times N}$ , where  $A_{i,j} = 1$  iff  $(v_i, v_j) \in \mathcal{E}$ . For simplicity, we also assume that  $G$  is undirected, i.e., that  $\mathbf{A}$  is symmetric. For each node  $v^{(i)} \in \mathcal{V}$  we have a feature vector  $\mathbf{x}^{(i)} \in \mathbb{R}^D$  and a label  $y^{(i)} \in \mathcal{Y}$ . The goal of the node classification task is to predict the label of each node in  $\mathcal{V}$ , given the graph structure and the node features.

GPNs classify the nodes of a given graph by first making a prediction for each node  $v^{(i)}$  solely based on its features  $\mathbf{x}^{(i)}$  using a standard PostNet model, i.e., without considering the graph structure. The predicted feature-based pseudo-count vectors  $\alpha^{\text{ft},(i)}$  for each vertex  $v^{(i)}$  are then dispersed through the graph via a *personalized Page-Rank* (PPR) matrix  $\mathbf{\Pi}^{\text{PPR}} \in \mathbb{R}^{N \times N}$  as follows:

$$\alpha^{\text{agg},(i)} := \sum_{v^{(j)} \in \mathcal{V}} \mathbf{\Pi}_{i,j}^{\text{PPR}} \alpha^{\text{ft},(j)} \quad (8)$$

$$\text{where } \mathbf{\Pi}^{\text{PPR}} := \left( \varepsilon \mathbf{I} + (1 - \varepsilon) \hat{\mathbf{A}} \right)^L \quad (9)$$

Here,  $\mathbf{I}$  is the identity matrix,  $\varepsilon \in (0, 1]$  the so-called *teleport probability*, and  $\hat{\mathbf{A}} := \mathbf{A} \mathbf{D}^{-1}$  the normalized (random-walk) adjacency matrix, with  $\mathbf{D} := \text{diag}(\mathbf{A} \mathbf{1})$  being the degree matrix of  $G$ . For large  $L$ ,  $\mathbf{\Pi}^{\text{PPR}}$  approximates the personalized page-rank matrix of the graph via power iteration. Gasteiger et al. [17] proposed this page-rank inspired information dispersion scheme for the node classification task, which they refer to as APPNP. The main difference between APPNP and GPN is that APPNP disperses (first-order) class probability vectors  $\theta^{\text{ft},(i)}$  for each node  $v^{(i)}$ , whereas GPN disperses pseudo-count vectors  $\alpha^{\text{ft},(i)}$ .

To justify this pseudo-count dispersion scheme, Stadler et al. [41] propose the following three axioms on how the structural information in a graph should influence the uncertainty of a model's predictions:

- A1** A node’s prediction should only depend on its own features in the absence of network effects. A node with features more different from training features should have a higher uncertainty.
- A2** All else being equal, if a node  $v^{(i)}$  has a lower epistemic uncertainty than its neighbors in the absence of network effects, the neighbors’ predictions should become less epistemically uncertain in the presence of network effects.
- A3** All else being equal, if a node  $v^{(i)}$  has a higher aleatoric uncertainty than its neighbors in the absence of network effects, the neighbors’ predictions should become more aleatorically uncertain in the presence of network effects. Further, the aleatoric uncertainty of a node in the presence of network effects should be higher if the predictions of its neighbors in the absence of network effects are more conflicting.

Stadler et al. [41] show the validity of those axioms if AU is defined as the least-confidence LConf and EU as the negative sum of the pseudo-counts  $EU_{PC}$  (Section 2.2). Using those definitions, the validity of the axioms follows from the fact that  $\alpha^{\text{agg.}(i)}$  is effectively a weighted average of the pseudo-counts of the (indirect) neighbors of  $v^{(i)}$ , with high weights for close neighbors and low weights for more distant ones. The GPN axioms are motivated by two assumptions, namely, *network homophily* and the *irreducibility of conflicts*.

First, *network homophily* refers to the assumption that an edge implies similarity of the connected nodes; more specifically, in the context of GPNs, connected nodes should have similar second-order distributions, and thereby similar predictive uncertainties. This is a common assumption shared by many GNN architectures and based on the idea of repeatedly summing or averaging the features of each node’s neighbors [26, 46]. As already remarked by Stadler et al. [41], non-homophilic graphs are not properly dealt with by GPNs, nor by other GNN architectures in general [49]. Nonetheless, since edges are typically used to represent some form of similarity, the homophily assumption is often reasonable.

Second, *irreducibility of conflicts* refers to the assumption that conflicting predictions cannot be resolved by aggregating the predictions of the conflicting nodes. Figure 1 illustrates the implications of this assumption for binary node classification; there, without network effects, node A is very confident that its probability of belonging to the positive class is high, whereas node B is very confident that its probability of belonging to that class is low. Thus, both nodes make conflicting predictions while both having a low AU and a low EU. Due to the homophily assumption, a consensus has to be found between the two conflicting predictions. As described in axiom **A3**, a GPN will do this by increasing the AU of the aggregated prediction while keeping the EU low. Stadler et al. [41] argue that this is reasonable because such a conflict is inherently irreducible and should therefore be reflected in the aleatoric uncertainty of the aggregated prediction.

### 3.3 GPN as an Opinion Pooling Model

In addition to the axiomatic motivation for the averaging of pseudo-counts, GPNs can also be interpreted from the perspective of *opinion pooling*. The ques-

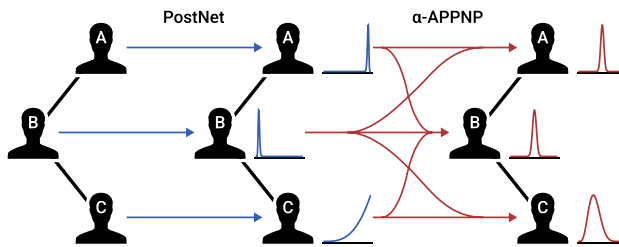


**Figure 1.** Illustration of how GPN aggregates the predictions (opinions) of different nodes (agents).

tion of how to pool, or aggregate, the opinions of multiple agents is studied in the fields of social choice theory [3] and decision and risk analysis [11, 12]. In the context of node classification, the agents are the nodes of the graph, and their opinions are the predicted second-order Dirichlet distributions. Figure 1 illustrates how GPN aggregates the distributions at different nodes. Let  $Q^{\text{ft},(i)} = \text{Dir}(\alpha^{\text{agg},(i)})$  be the distribution at node  $v^{(i)}$  before dispersion and  $Q^{\text{agg},(i)} = \text{Dir}(\alpha^{\text{agg},(i)})$  the distribution after dispersion. We can then express the aggregated distribution  $Q^{\text{agg},(i)}$  as follows:

$$\begin{aligned}
 Q^{\text{agg},(i)}(\theta) &= \frac{1}{B(\alpha^{\text{agg},(i)})} \prod_{k=1}^K \theta_k^{\alpha_k^{\text{agg},(i)} - 1} = \frac{1}{B(\alpha^{\text{agg},(i)})} \prod_{k=1}^K \theta_k^{(\sum_{j=1}^N \Pi_{i,j}^{\text{PPR}} \alpha_k^{\text{ft},(j)}) - 1} \\
 &= \underbrace{\frac{\prod_{j=1}^N (B(\alpha^{\text{ft},(j)})) \Pi_{i,j}^{\text{PPR}}}{B(\alpha^{\text{agg},(i)})}}_{Z^{-1}} \prod_{j=1}^N \left( \frac{1}{B(\alpha^{\text{ft},(j)})} \prod_{k=1}^K \theta_k^{\alpha_k^{\text{ft},(j)} - 1} \right)^{\Pi_{i,j}^{\text{PPR}}} \\
 &= \frac{1}{Z} \prod_{j=1}^N (Q^{\text{ft},(j)}(\theta))^{\Pi_{i,j}^{\text{PPR}}} \quad \text{with } Z = \int_{\Delta_K} \prod_{j=1}^N (Q^{\text{ft},(j)}(\theta))^{\Pi_{i,j}^{\text{PPR}}} d\theta
 \end{aligned} \tag{10}$$

Here,  $B(\cdot)$  denotes the (multivariate) Beta function and  $Z$  a normalization constant. This formulation of the aggregated distribution  $Q^{\text{agg},(i)}$  in terms of the distributions  $Q^{\text{ft},(j)}$  of the neighbors of  $v^{(i)}$  is called *log-linear opinion pooling* (LLOP) [12, 18, 19, 27]. LLOP is a natural opinion pooling scheme which is typically motivated by the fact that it satisfies so-called *external Bayesianity* [18], i.e., applying a Bayesian update to the pooled opinion is equivalent to applying that update to all opinions before pooling. In the context of Dirichlet opinions, external Bayesianity simply refers to the fact that adding a pseudo-count vector  $\gamma \in \mathbb{R}_{\geq 0}^K$  to the aggregated pseudo-count vector  $\alpha^{\text{agg},(i)}$  results in the same aggregated distribution as adding  $\gamma$  to each of the pseudo-count vectors  $\alpha^{\text{ft},(j)}$  of the neighbors of  $v^{(i)}$  and then aggregating. Additionally, Abbas [1] has shown that  $Q^{\text{agg},(i)}$  minimizes the expected KL divergence  $\sum_{j=1}^N \Pi_{i,j}^{\text{PPR}} D_{\text{KL}}(Q^{\text{agg},(i)} \| Q^{\text{ft},(j)})$ .

To summarize, GPN can be understood as an opinion pooling model based on the LLOP scheme. Since there is a large variety of pooling schemes [27], this raises the question of whether LLOP is the most appropriate opinion pooling scheme for the node classification task.

## 4 Committee-based Graph Uncertainty Quantification

In this section, we propose a new family of models, called *Committee-based Uncertainty Quantification Graph Neural Network* (CUQ-GNN), which combines standard GNNs with the PostNet model. We first discuss the validity of LLOP scheme employed by GPNs and identify limitations of this approach. Next, we show how those limitations can be addressed by so-called *behavioral pooling* schemes. Last, CUQ-GNN is introduced as a concrete instantiation of this idea.

### 4.1 The Irreducibility of Conflicts Assumption

As explained in Section 3.2, GPNs are based on the assumption that conflicts between the predictions of neighboring nodes are irreducible. In a recent work, we argued [13] that the validity of this *irreducibility* assumption depends on the nature of the data-generating process which produces the graph whose nodes are to be classified. We will now describe this argument since it serves as motivation the CUQ-GNN model introduced in the next section. As mentioned in the introduction, irreducibility in the context of UQ refers to uncertainty that cannot be reduced by additional information, which, in a machine learning context, essentially means sampling additional data [23]. In the context of node classification, the data points are nodes; given a sample graph  $G_N = (\mathcal{V}_N, \mathcal{E}_N)$  with  $N$  vertices, increasing the sample size corresponds to sampling a graph  $G_M = (\mathcal{V}_M, \mathcal{E}_M)$  with  $M > N$  nodes from an assumed underlying data-generating distribution  $P_{\mathcal{G}}$  over all graphs  $\mathcal{G}$ , such that  $G_N$  is a subgraph of  $G_M$ . The question of whether a conflict between a node  $v^{(i)}$  and its neighbor  $v^{(j)}$  is irreducible then becomes the question of whether the conflict persists in the limit of  $M \rightarrow \infty$ . Let  $\mathcal{N}_M(v^{(i)})$  be the set of neighbors of  $v^{(i)}$  in  $G_M$ . Assuming homophily, each node  $v^{(\ell)}$  that is added to  $\mathcal{N}_M(v^{(i)})$  should be *similar* to  $v^{(i)}$  with high probability. Depending on the data-generating distribution  $P_{\mathcal{G}}$ , there are two possible scenarios:

1. **Bounded degree sampling:** The neighborhood of  $v^{(i)}$  does not grow with the sample size, i.e.,  $\mathbb{E}[|\mathcal{N}_M(v^{(i)})|] \in \mathcal{O}(1)$  as  $M \rightarrow \infty$ . In this situation, the conflict between  $v^{(i)}$  and  $v^{(j)}$  is indeed irreducible, as no additional data can be sampled to resolve the conflict. Thus, axiom **A3** of GPN is reasonable, the irreducible uncertainty, i.e., AU, should increase with conflicting predictions.
2. **Unbounded degree sampling:** The neighborhood of  $v^{(i)}$  grows with the sample size, i.e.,  $\mathbb{E}[|\mathcal{N}_M(v^{(i)})|] \rightarrow \infty$  as  $M \rightarrow \infty$ . In this situation, the conflict is reducible, as it will eventually be resolved by the addition of more similar nodes to the neighborhood of  $v^{(i)}$ , which will outweigh the conflicting node  $v^{(j)}$ . Thus, the conflict resolution approach of GPN is not reasonable; not AU, but rather the reducible uncertainty, EU, should increase.



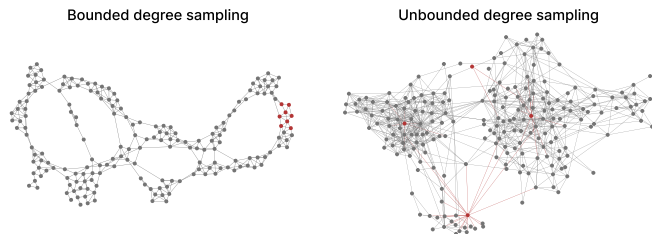


**Figure 2.** Examples for graphs obtained via bounded and unbounded degree sampling.

We argue that unbounded degree sampling is more common in practical node classification tasks. The Barabási-Albert model [4] is a scale-free model which describes the growth behavior of many real-world graphs, such as the World Wide Web, social networks, or citation networks [2, 36, 43]. In this model, the expected degree of the  $N$ -th sampled node  $v^{(i)}$  after  $M - N$  additional nodes have been sampled is equal to  $|\mathcal{N}_N(v^{(i)})| \cdot \sqrt{\frac{M}{N}}$ . Thus, for  $M \rightarrow \infty$ , the expected neighborhood size of a node goes to infinity. Examples of domains in which the neighborhood sizes do not grow with the size of a graph are molecular graphs or lattice graphs, such as 3D models or images, which can be interpreted as grids of pixels (see Fig. 2). In those domains, node-level classification tasks are however less common, as one is typically interested in the classification of entire graphs, e.g., whether a given molecule is toxic or not.

To conclude, we argue that the axiomatic motivation for GPNs is oftentimes inappropriate. Therefore, we propose a different approach to UQ for node classification which does not assume the irreducibility of conflicts from axiom **A3**.

## 4.2 Resolving Conflicts via Behavioral Pooling

The LLOP scheme employed by GPNs is a so-called *axiomatic pooling* approach [12]. As described in the previous section, this axiomatic pooling scheme may not be appropriate if the domain does not satisfy the bounded degree sampling assumption. For domains in which the unbounded degree sampling assumption holds, the so-called LOP-GPN model [13] has been shown to be a more appropriate choice. As the name suggests, LOP-GPN is a variant of GPN that uses the axiomatic *linear opinion pooling* (LOP) scheme instead of LLOP. LOP combines distributions by taking a weighted average of their densities, i.e.,  $Q^{\text{agg},(i)} = \sum_{v^{(j)} \in \mathcal{V}} \Pi_{i,j}^{\text{PPR}} Q^{\text{ft},(j)}$  (cf. Eq. (10)). However, due to the inherent variability of real-world node classification tasks, it is difficult to determine a priori whether a given domain satisfies the bounded or unbounded degree sampling assumptions. In practice, a domain might even exhibit a mixture of both sampling behaviors in different regions of a given graph. Whether and when a local conflict in a graph is irreducible is a complex question that depends on the domain and its inherent data-generating distribution. While the axiomatic motivations for GPN and LOP-GPN are appealing in theory, it is difficult to determine whether

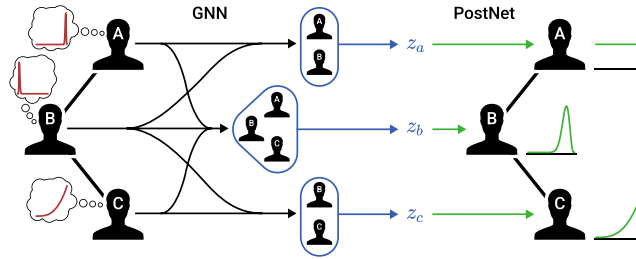


**Figure 3.** Illustration of how CUQ-GNN can flexibly resolve conflicts.

they are appropriate for a given problem. Therefore, we argue that the appropriateness of a given UQ approach can only be meaningfully assessed by empirically comparing the quality and usefulness of the uncertainty estimates the produce.

This uncertainty about the appropriateness of different pooling schemes, motivates the idea of learning a pooling scheme from the data. By giving up the theoretical guarantees about the properties of uncertainty estimates that axiomatic pooling schemes provide, a so-called *behavioral pooling* approach can more flexibly adapt to the specific characteristics of a given task [11]. While axiomatic pooling schemes combine the independent opinions of agents using a fixed aggregation rule, behavioral pooling schemes permit interactions between the agents. All agents (nodes) that interact with a given agent  $v^{(i)}$  can be interpreted as a group, or committee,  $C^{(i)} \subseteq \mathcal{V}$  of agents which directly produces a joint opinion about  $v^{(i)}$ . Figure 3 illustrates this idea. In Fig. 1, the conflict between node A and B increases the pooled AU; by allowing A and B to exchange information, such a conflict can be resolved more flexibly, e.g., by predicting a uniform second-order distribution and thereby increasing EU.

A behavioral pooling scheme is defined by two aspects: First, the way the committees  $C^{(i)}$  are constructed and, second, the way the agents within a committee interact. A graph convolution, as used in GNNs, can be interpreted as such a behavioral pooling scheme, where  $C^{(i)}$  is defined as a (indirect or higher-order) neighborhood of  $v^{(i)}$  and the interaction between the agents is defined by the learned aggregation mechanism of the convolution operator. There is a large variety of graph convolution operators in the literature, each defining a different way of constructing the committees and agent interactions.

Most common graph convolutions are based on the idea of neighborhood message-passing; a stack of  $L$  graph convolution layers can be interpreted as a behavioral pooling scheme, where the committees  $C^{(i)}$  are defined as the  $L$ -hop neighborhoods of  $v^{(i)}$ . Examples of such neighborhood message-passing convolutions are APPNP [17], *Graph Convolutional Network* (GCN) [26] and *Graph Attention Network* (GAT) [42]. Alternatively, there are also so-called higher-order convolutions [14, 31], which do not operate directly on node features but on more complex substructures of a graph. While the homophily assumption of GPN is also (implicitly) made in many graph convolution operators, so-called heterogeneous graph convolutions [44, 47] do not make this assumption. Overall,

different types of graph convolutions have been successfully employed on a wide range of tasks on graph data.

We propose a simple extension of graph convolutions to the UQ setting by combining them with the PostNet model [10]. We call this combination *CUQ-GNN*:

$$\text{CUQ-GNN}(\mathbf{X}, \mathbf{A}) = \text{PostNet}(\text{GNN}(h_{enc}(\mathbf{X}), \mathbf{A}) \cdot \mathbf{W}_{lat}) \quad (11)$$

Here,  $\mathbf{X} \in \mathbb{R}^{N \times d_m}$  is the input node feature matrix,  $\mathbf{A} \in \mathbb{R}^{N \times N}$  the adjacency matrix,  $h_{enc} : \mathbb{R}^{N \times d_m} \rightarrow \mathbb{R}^{N \times d_{hid}}$  a *multilayer perceptron*,  $\text{GNN} : \mathbb{R}^{N \times d_{hid}} \times \mathbb{R}^{N \times N} \rightarrow \mathbb{R}^{N \times d_{hid}}$  a stack of graph convolution operators,  $\mathbf{W}_{lat} \in \mathbb{R}^{d_{hid} \times d_{lat}}$  a latent embedding matrix and  $\text{PostNet} : \mathbb{R}^{N \times d_{lat}} \rightarrow \mathbb{R}_{\geq 1}^{N \times K}$  a PostNet model.

By choosing an appropriate graph convolution operator, CUQ-GNN can be applied to a wide range of node classification tasks. Unlike GPN, CUQ-GNN neither assumes homophily nor the irreducibility of conflicts. This flexibility comes at the cost of having no provable guarantees about the uncertainty estimates. Nevertheless, due to the questionable real-world applicability of the axioms of GPN, we argue that giving up (potentially) invalid axioms for a more flexible propagation of uncertainties through the graph is a justifiable trade-off.

## 5 Evaluation

We assess the quality of the uncertainty estimates of CUQ-GNN in two ways. First, we compare the quality of uncertainty estimates of different CUQ-GNN variants and GPN using *accuracy-rejection curves* (ARCs). Second, we compare the effectiveness of uncertainty estimates in detecting anomalous instances in two *out-of-distribution* (OOD) settings. All experiments are conducted on six common node classification benchmarks.<sup>3</sup>

### 5.1 Experimental Setup

*Datasets* We use the following node classification benchmarks: Three citation network datasets, namely, **CoramL**, **CiteSeer** and **PubMed** [20, 21, 33, 34, 38], two co-purchase datasets, namely **Amazon Photos** and **Amazon Computers** [32] and the large-scale **OGBN Arxiv** dataset with about 170k nodes and over 2.3 million edges [22]. Since OGBN Arxiv is presplit into train, validation and test sets, we use the provided splits. The results for the other datasets are obtained by averaging over 10 random class-stratified splits of the node set with train/val/test sizes of 5%/15%/80%.

*Models* We evaluate three variants of CUQ-GNN: **CUQ-PPR**, **CUQ-GCN** and **CUQ-GAT**. CUQ-PPR uses APPNP [17], CUQ-GCN uses GCN [26] and CUQ-GAT uses GAT convolutions [42]. Note that those three convolution operators are homogeneous, i.e., they assume an homophilic input graph. This

<sup>3</sup> Implementation available at <https://github.com/Cortys/gpn-extensions>

choice was made because most node classification datasets, including the chosen benchmark datasets, satisfy the homophily assumption. The three CUQ-GNN variants are compared against the following four baseline models: The standard **GPN** model using LLOP [41], **LOP-GPN** which uses LOP [13], the first-order **APPNP** model [17] and the parameter-free *Graph-based Kernel Dirichlet distribution Estimation* (**GKDE**) model [48]. The hyperparameters and the training schedules for the models are chosen as described by Stadler et al. [41]. The sizes and parameters of  $h_{enc}$ ,  $\mathbf{W}_{lat}$  and the PostNet model in CUQ-GNN (Eq. (11)) are chosen as in the GPN model [41]. For CUQ-PPR, the APPNP convolution model is parameterized like the standalone APPNP model, i.e.,  $L = 10$  power iteration steps and a teleport probability of  $\varepsilon = 0.1$  (Eq. (9)). For CUQ-GCN and CUQ-GAT, the GNN models consist of two convolution layers. For GCN, ReLU is used as activation function; for GAT, we use a single attention head with an *Exponential Linear Unit* activation between the convolution layers.

*Evaluation Metrics* We assess the quality of the following five uncertainty estimates: The entropy-based TU, AU and EU (Eqs. (2) to (4)), the pseudo-count based  $EU_{PC}$  (Section 2.2) and the second-order epistemic uncertainty  $EU_{SO}$  (Eq. (5)). Since APPNP only produces first-order predictions, we only evaluate the TU of this model. All other models predict second-order Dirichlet distributions and are evaluated using all four uncertainty estimates.

## 5.2 Accuracy-Rejection Curves

We begin with a comparison of CUQ-GNN and GPN using so-called *accuracy-rejection curves* (ARCs). The curves show the test accuracies of each model when discarding all test instances below a given uncertainty threshold. For an uncertainty measure that captures predictive uncertainty well, the accuracy should monotonically increase with the rejection rate and, ideally, approach 100%. Figure 4 shows the ARCs of GPN and the three evaluated CUQ-GNN variants using the entropy-based TU and EU measures and the pseudo-count based  $EU_{PC}$ .

The accuracy of the CUQ-GNN models when looking at the entire dataset, i.e., at 0% rejection, is either close to or significantly higher than that of, both, GPN and LOP-GPN. While CUQ-GNN is motivated by the idea of behavioral pooling to resolve conflicts between nodes more flexibly and thereby improve its uncertainty estimates, the increased flexibility also improves the model’s generalization performance in general. Within the three evaluated types of CUQ-GNN models, there is no clear winner across all datasets, supporting the idea that the appropriateness of a given pooling mechanism is highly domain-dependent.

As should be expected, accuracy increases monotonically with increasing rejection rates across all uncertainty measures, models, and datasets. Additionally, all CUQ-GNN variants reach accuracies close to 100% as the rejection rate increases. For GPN, on the other hand, the delta to 100% at high rejection rates is significantly higher. There are two notable exceptions to those observations: First, the ARCs of CUQ-PPR are nearly flat on the Amazon Photos and Amazon Computers datasets when using entropy-based EU. Using pseudo-count-based

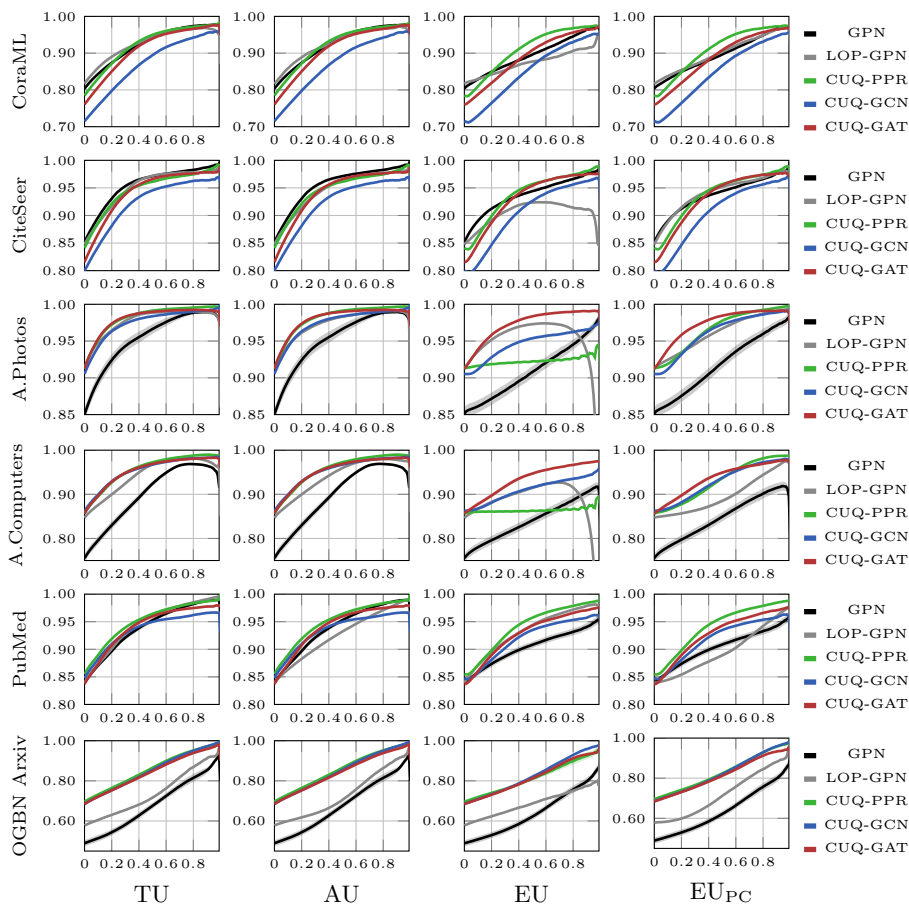


**Figure 4.** Accuracy-rejection curve for different uncertainty measures. The x-axis represents the fraction of rejected test instances; the y-axis represents the test accuracy for a given rejection rate. The (small) shaded areas behind the curves represent the estimate’s standard error.

EUs, the ARC of CUQ-PPR on those datasets is, however, increasing. This discrepancy illustrates the previously mentioned problem that entropy-based measures are not always appropriate measures of uncertainty [45]. Second, using the entropy-based TU, AU and EU measures, the ARCs of GPN and LOP-GPN go down for high rejection rates on the two Amazon datasets, indicating that the models incorrectly assign high confidences to wrong predictions.

To summarize, Fig. 4 shows that **CUQ-GNN achieves a similar or better predictive performance than GPN and LOP-GPN**. Additionally, the **uncertainty estimates of CUQ-GNN behave better than those of GPN and LOP-GPN**, in the sense that they lead to near-perfect accuracies at high rejection rates.

Table 1. OOD detection performance of OOD vs ID vertices and ID accuracies.

		Leave-out Classes						$\mathbf{x}^{(v)} \sim \mathcal{N}(0, 1)$					
		ID Acc	TU	OOD-AUC-ROC			EU <sub>SO</sub>	ID Acc	TU	OOD-AUC-ROC			EU <sub>SO</sub>
				AU	EU	EU <sub>PC</sub>				AU	EU	EU <sub>PC</sub>	
CoraML	APPNP	<b>90.44</b>	<b>87.45</b>	-	-	-	-	43.62	13.26	-	-	-	-
	GKDE	83.01	77.21	35.35	69.16	74.00	76.46	71.96	48.71	50.76	49.19	48.45	48.68
	GN	89.36	85.51	85.49	<b>86.23</b>	<b>87.11</b>	<b>89.15</b>	17.86	<b>96.59</b>	<b>96.80</b>	70.89	70.62	75.66
	LOP-GPN	89.34	85.67	<b>88.51</b>	45.18	84.72	79.26	<b>81.74</b>	69.50	61.06	82.08	60.15	83.69
	CUQ-PPR	87.81	81.18	81.20	78.10	78.23	80.37	26.85	85.28	53.09	<b>89.97</b>	<b>91.24</b>	<b>88.23</b>
	CUQ-GCN	82.42	74.41	74.44	69.23	69.27	72.47	27.47	75.03	57.37	78.97	80.28	77.57
	CUQ-GAT	85.97	79.88	79.88	78.10	78.10	79.86	30.56	69.76	60.79	71.10	71.40	70.66
CiteSeer	APPNP	<b>87.75</b>	<b>85.80</b>	-	-	-	-	72.72	23.76	-	-	-	-
	GKDE	73.73	77.89	37.03	65.08	<b>81.30</b>	79.44	65.79	50.14	51.33	48.80	50.17	50.04
	GN	87.23	81.53	<b>81.52</b>	76.78	76.76	<b>80.62</b>	17.45	93.00	<b>93.22</b>	80.32	79.91	86.34
	LOP-GPN	87.16	82.19	80.57	73.09	75.48	73.12	<b>84.41</b>	81.65	76.92	81.26	59.20	86.81
	CUQ-PPR	86.41	79.39	79.42	76.34	76.34	77.50	60.71	<b>94.61</b>	78.28	<b>94.82</b>	<b>94.84</b>	<b>94.71</b>
	CUQ-GCN	82.63	72.32	72.48	67.17	67.15	69.78	52.64	90.50	79.52	91.25	91.30	90.82
	CUQ-GAT	83.00	79.10	80.11	<b>77.48</b>	77.48	78.43	54.77	86.00	77.26	87.10	87.12	86.81
Amazon Photos	APPNP	<b>94.99</b>	75.12	-	-	-	-	40.44	13.17	-	-	-	-
	GKDE	85.45	70.20	55.45	61.23	60.80	66.83	76.19	49.07	50.74	48.76	48.87	48.95
	GN	91.49	76.29	76.29	<b>86.54</b>	<b>87.50</b>	<b>86.05</b>	12.63	89.43	<b>91.07</b>	60.06	59.86	63.56
	LOP-GPN	94.00	<b>86.50</b>	<b>83.88</b>	80.02	76.63	83.87	<b>91.18</b>	<b>91.76</b>	87.29	89.36	61.15	<b>95.74</b>
	CUQ-PPR	92.76	75.18	75.19	65.17	69.96	72.69	20.75	89.93	58.20	<b>93.41</b>	<b>93.37</b>	89.38
	CUQ-GCN	92.26	76.11	76.12	69.44	69.81	72.58	15.74	62.53	50.99	65.94	65.80	61.89
	CUQ-GAT	92.69	78.82	78.82	76.79	76.87	78.13	23.00	62.11	59.52	62.66	62.65	62.07
Amazon Computers	APPNP	87.99	79.32	-	-	-	-	42.81	15.58	-	-	-	-
	GKDE	71.26	76.38	70.52	74.46	74.37	76.20	64.01	49.92	49.81	50.03	50.09	49.99
	GN	82.17	79.17	79.17	<b>76.65</b>	<b>81.01</b>	83.77	16.39	88.69	89.62	62.32	62.12	65.90
	LOP-GPN	90.28	<b>85.00</b>	<b>88.08</b>	68.40	77.98	<b>83.80</b>	<b>84.49</b>	<b>94.76</b>	<b>90.93</b>	88.33	65.30	<b>98.15</b>
	CUQ-PPR	90.53	72.78	72.78	50.65	61.73	66.21	24.02	86.02	41.73	<b>89.86</b>	<b>90.44</b>	84.00
	CUQ-GCN	<b>91.87</b>	68.34	68.34	59.46	60.06	62.51	13.06	60.39	49.91	62.43	62.94	58.91
	CUQ-GAT	91.81	79.74	79.78	75.31	75.57	76.91	16.14	58.25	57.18	58.41	58.44	58.16
PubMed	APPNP	<b>94.59</b>	69.38	-	-	-	-	59.59	10.95	-	-	-	-
	GKDE	87.93	<b>71.51</b>	39.69	65.30	69.74	71.00	76.96	49.94	50.16	49.79	49.87	49.93
	GN	93.76	69.87	<b>69.85</b>	<b>72.95</b>	<b>72.93</b>	<b>73.62</b>	30.29	<b>95.74</b>	<b>96.41</b>	70.52	70.29	76.44
	LOP-GPN	93.23	68.96	69.10	66.28	64.87	64.30	<b>83.99</b>	82.71	75.93	80.37	67.74	91.84
	CUQ-PPR	94.28	65.19	65.19	64.19	64.15	65.22	44.25	91.93	59.89	<b>93.18</b>	<b>93.45</b>	<b>92.97</b>
	CUQ-GCN	94.03	61.88	62.35	59.61	59.62	61.09	45.53	81.47	61.04	83.07	83.69	82.65
	CUQ-GAT	92.86	63.32	64.40	59.09	59.07	61.98	46.02	69.93	61.10	70.81	71.06	70.66
OGBN Arxiv	APPNP	73.33	64.47	-	-	-	-	<b>66.53</b>	42.63	-	-	-	-
	GKDE	60.04	68.69	66.97	66.70	67.46	68.14	56.91	49.52	49.55	49.48	49.47	49.46
	GN	55.36	67.08	67.08	66.92	66.91	68.79	4.35	77.08	77.45	67.14	66.92	69.93
	LOP-GPN	63.37	66.77	68.12	54.58	66.28	67.44	57.49	82.46	73.03	87.08	68.39	92.39
	CUQ-PPR	<b>74.38</b>	68.58	68.58	60.96	66.73	68.32	52.17	<b>86.16</b>	<b>86.12</b>	<b>93.54</b>	<b>93.59</b>	<b>93.25</b>
	CUQ-GCN	73.56	68.29	68.28	67.82	67.84	68.98	30.20	69.93	69.85	75.65	75.65	75.00
	CUQ-GAT	73.21	<b>69.05</b>	<b>69.05</b>	<b>68.40</b>	<b>68.40</b>	<b>69.65</b>	62.11	58.34	58.33	61.55	61.55	60.92

### 5.3 OOD Detection

One practical application of UQ is the detection of outliers, i.e., distinguishing nodes that are in the data distribution from those that lie *out-of-distribution* (OOD). Similar to Stadler et al. [41], we generate outlier nodes in two ways:

1. Nodes belonging to a pre-selected subset of classes are omitted from the training data; during testing, a model should then detect nodes from the unseen classes as outliers.
2. The features of a random subset of test nodes are altered by adding Gaussian noise to them; a model should detect the noisy nodes as outliers.

The performance of a given uncertainty measure is assessed via the *area under the receiver operating characteristic curve* (AUC-ROC). Table 1 shows the OOD detection performances and the *in-distribution* (ID) accuracies on both OOD detection scenarios. Note that standard errors were omitted because they are close to zero for all entries.

Looking at the ID accuracies, APPNP generally performs best in the leave-out classes scenario, while LOP-GPN performs best in the Gaussian noise sce-

nario. Note, however, that the difference between the ID accuracies of APPNP and CUQ-PPR in the leave-out classes scenario is relatively small; this similarity is plausible since CUQ-PPR can be seen as a second-order, uncertainty-aware variant of APPNP.

Comparing the OOD detection performance of different models, CUQ-GNN, more specifically CUQ-PPR, achieves the best AUC-ROC values most often in the Gaussian noise scenario, followed by GPN and LOP-GPN. In the leave-out classes scenario GPN achieves the best result most often, followed by CUQ-GAT and LOP-GPN. This shows that, depending on the setting, both, the behavioral pooling of CUQ-GNN and the axiomatic approaches of (LOP-)GPN are well-suited for outlier detection problems. To summarize, **the well-behaved ARCs of CUQ-GNNs observed in the previous section also translate into a good practical performance on OOD tasks.**

## 6 Conclusion

In this paper, we proposed the family of CUQ-GNN models for uncertainty quantification in node classification. Unlike GPN and LOP-GPN, which employ static axiomatic pooling schemes, CUQ-GNN is based on the more flexible notion of behavioral pooling from the field of risk and decision analysis. More specifically, behavioral pooling is realized by combining standard graph convolution operators with a PostNet model. We demonstrate the effectiveness of our approach empirically by comparing it to multiple state-of-the-art baseline methods.

We envision three lines of future research. First, a deeper and more systematic investigation of the intersection of opinion pooling and uncertainty propagation on graphs would be desirable. While our proposed behavioral pooling approach achieves strong empirical results, it does not provide theoretical guarantees for its uncertainty estimates. Second, as we have seen, choosing an appropriate graph convolution operator for CUQ-GNN is a complex domain-dependent problem. Therefore, it would be interesting to design an AutoML system to automatically configure CUQ-GNN for a given domain. Third, GPN, LOP-GPN and CUQ-GNN are all only applicable to node classification tasks. Extending this line of work to graph classification or node regression tasks would be interesting as well.

**Disclosure of Interests.** The authors have no competing interests to declare that are relevant to the content of this article.

## References

1. Abbas, A.E.: A Kullback-Leibler View of Linear and Log-Linear Pools. *Decision Analysis* **6**(1), 25–37 (2009)
2. Albert, R., Barabási, A.L.: Statistical mechanics of complex networks. *Rev. Mod. Phys.* **74**(1), 47–97 (2002)
3. Arrow, K.J.: *Social Choice and Individual Values*. Wiley: New York (1951)
4. Barabási, A.L., Albert, R.: Emergence of Scaling in Random Networks. *Science* **286**(5439), 509–512 (1999)

5. Bengs, V., Hüllermeier, E., Waegeman, W.: Pitfalls of Epistemic Uncertainty Quantification through Loss Minimisation. *NeurIPS* **35**, 29205–29216 (2022)
6. Bengs, V., Hüllermeier, E., Waegeman, W.: On Second-Order Scoring Rules for Epistemic Uncertainty Quantification. In: *ICML*, pp. 2078–2091, PMLR (2023)
7. Biloš, M., Charpentier, B., Günnemann, S.: Uncertainty on Asynchronous Time Event Prediction. In: *NeurIPS*, vol. 32 (2019)
8. Bojchevski, A., Günnemann, S.: Deep Gaussian Embedding of Graphs: Unsupervised Inductive Learning via Ranking. In: *ICLR* (2018)
9. Bronevich, A., Klir, G.J.: Axioms for uncertainty measures on belief functions and credal sets. In: *NAFIPS 2008*, pp. 1–6 (2008)
10. Charpentier, B., Zügner, D., Günnemann, S.: Posterior network: Uncertainty estimation without OOD samples via density-based pseudo-counts. In: *NeurIPS* (2020)
11. Clemen, R.T., Winkler, R.L.: Combining Probability Distributions From Experts in Risk Analysis. *Risk Anal* **19**(2), 187–203 (1999)
12. Clemen, R.T., Winkler, R.L.: Aggregating Probability Distributions. In: *Advances in Decision Analysis: From Foundations to Applications*, pp. 154–176 (2007)
13. Damke, C., Hüllermeier, E.: Linear Opinion Pooling for Uncertainty Quantification on Graphs. In: *UAI’2024, Barcelona* (2024)
14. Damke, C., Melnikov, V., Hüllermeier, E.: A Novel Higher-order Weisfeiler-Lehman Graph Convolution. In: *ACML*, pp. 49–64, PMLR (2020)
15. Depeweg, S., Hernandez-Lobato, J.M., Doshi-Velez, F., Udluft, S.: Decomposition of Uncertainty in Bayesian Deep Learning for Efficient and Risk-sensitive Learning. In: *ICML*, pp. 1184–1193, PMLR (2018)
16. Duan, R., Caffo, B., Bai, H.X., Sair, H.I., Jones, C.: Evidential Uncertainty Quantification: A Variance-Based Perspective. In: *WACV* (2024)
17. Gasteiger, J., Bojchevski, A., Günnemann, S.: Predict then Propagate: Graph Neural Networks meet Personalized PageRank. In: *ICLR* (2018)
18. Genest, C.: A Characterization Theorem for Externally Bayesian Groups. *The Annals of Statistics* **12**(3), 1100–1105 (1984)
19. Genest, C., Zidek, J.V.: Combining Probability Distributions: A Critique and an Annotated Bibliography. *Statistical Science* **1**(1), 114–135 (1986)
20. Getoor, L.: Link-based Classification. In: Bandyopadhyay, S., Maulik, U., Holder, L.B., Cook, D.J. (eds.) *Advanced Methods for Knowledge Discovery from Complex Data*, pp. 189–207, Springer (2005)
21. Giles, C.L., Bollacker, K.D., Lawrence, S.: CiteSeer: An automatic citation indexing system. In: *Third ACM Conference on Digital Libraries*, pp. 89–98 (1998)
22. Hu, W., Fey, M., Zitnik, M., Dong, Y., Ren, H., Liu, B., Catasta, M., Leskovec, J.: Open Graph Benchmark: Datasets for Machine Learning on Graphs. In: *NeurIPS*, vol. 33, pp. 22118–22133 (2020)
23. Hüllermeier, E., Waegeman, W.: Aleatoric and epistemic uncertainty in machine learning: An introduction to concepts and methods. *Mach Learn* **110**(3) (2021)
24. Huseljic, D., Sick, B., Herde, M., Kottke, D.: Separation of Aleatoric and Epistemic Uncertainty in Deterministic Deep Neural Networks. In: *ICPR’2020* (2021)
25. Kendall, A., Gal, Y.: What uncertainties do we need in Bayesian deep learning for computer vision? In: *NeurIPS*, pp. 5580–5590, Curran Associates Inc. (2017)
26. Kipf, T.N., Welling, M.: Semi-Supervised Classification with Graph Convolutional Networks. In: *ICLR* (2017)
27. Koliander, G., El-Laham, Y., Djurić, P.M., Hlawatsch, F.: Fusion of Probability Density Functions. *IEEE* **110**(4), 404–453 (2022)



28. Kopetzki, A.K., Charpentier, B., Zügner, D., Giri, S., Günnemann, S.: Evaluating Robustness of Predictive Uncertainty Estimation: Are Dirichlet-based Models Reliable? In: ICML, pp. 5707–5718, PMLR (2021)
29. Kotelevskii, N., Horváth, S., Nandakumar, K., Takáč, M., Panov, M.: Dirichlet-based Uncertainty Quantification for Personalized Federated Learning with Improved Posterior Networks (2023)
30. Malinin, A., Gales, M.: Predictive uncertainty estimation via prior networks. In: NeurIPS, pp. 7047–7058, Curran Associates Inc. (2018)
31. Maron, H., Ben-Hamu, H., Serviansky, H., Lipman, Y.: Provably Powerful Graph Networks. arXiv (2019)
32. McAuley, J., Targett, C., Shi, Q., van den Hengel, A.: Image-Based Recommendations on Styles and Substitutes. In: 38th International ACM SIGIR Conference on Research and Development in Information Retrieval, pp. 43–52 (2015)
33. McCallum, A.K., Nigam, K., Rennie, J., Seymore, K.: Automating the Construction of Internet Portals with Machine Learning. *Information Retrieval* **3**(2) (2000)
34. Namata, G., London, B., Getoor, L., Huang, B.: Query-driven Active Surveying for Collective Classification. In: MLG Workshop (2012)
35. Pal, N.R., Bezdek, J.C., Hemasinha, R.: Uncertainty measures for evidential reasoning II: A new measure of total uncertainty. *IJAR* **8**(1), 1–16 (1993)
36. Redner, S.: How popular is your paper? An empirical study of the citation distribution. *Eur. Phys. J. B* **4**(2), 131–134 (1998)
37. Sale, Y., Hofman, P., Wimmer, L., Hüllermeier, E., Nagler, T.: Second-Order Uncertainty Quantification: Variance-Based Measures (2023)
38. Sen, P., Namata, G., Bilgic, M., Getoor, L., Galligher, B., Eliassi-Rad, T.: Collective Classification in Network Data. *AI Magazine* **29**(3), 93–93 (2008)
39. Sensoy, M., Kaplan, L., Kandemir, M.: Evidential deep learning to quantify classification uncertainty. In: NeurIPS, pp. 3183–3193, Curran Associates Inc. (2018)
40. Shu, K., Sliva, A., Wang, S., Tang, J., Liu, H.: Fake News Detection on Social Media: A Data Mining Perspective. *SIGKDD Explor. Newsl.* **19**(1), 22–36 (2017)
41. Stadler, M., Charpentier, B., Geisler, S., Zügner, D., Günnemann, S.: Graph Posterior Network: Bayesian Predictive Uncertainty for Node Classification (2021)
42. Veličković, P., Cucurull, G., Casanova, A., Romero, A., Liò, P., Bengio, Y.: Graph Attention Networks. In: ICLR (2018)
43. Wang, M., Yu, G., Yu, D.: Measuring the preferential attachment mechanism in citation networks. *Physica A: Stat Mechanics and its Applications* **387**(18) (2008)
44. Wang, X., Ji, H., Shi, C., Wang, B., Ye, Y., Cui, P., Yu, P.S.: Heterogeneous Graph Attention Network. In: The World Wide Web Conference, pp. 2022–2032 (2019)
45. Wimmer, L., Sale, Y., Hofman, P., Bischl, B., Hüllermeier, E.: Quantifying aleatoric and epistemic uncertainty in machine learning: Are conditional entropy and mutual information appropriate measures? In: UAI’2023, pp. 2282–2292, PMLR (2023)
46. Xu, K., Hu, W., Leskovec, J., Jegelka, S.: How Powerful are Graph Neural Networks? In: ICLR (2018)
47. Zhang, C., Song, D., Huang, C., Swami, A., Chawla, N.V.: Heterogeneous Graph Neural Network. In: 25th ACM SIGKDD International Conference on Knowledge Discovery & Data Mining, pp. 793–803 (2019)
48. Zhao, X., Chen, F., Hu, S., Cho, J.H.: Uncertainty aware semi-supervised learning on graph data. In: NeurIPS, pp. 12827–12836, Curran Associates Inc. (2020)
49. Zhu, J., Yan, Y., Zhao, L., Heimann, M., Akoglu, L., Koutra, D.: Beyond homophily in graph neural networks: Current limitations and effective designs. In: NeurIPS, pp. 7793–7804, Curran Associates Inc. (2020)